

We are IntechOpen, the world's leading publisher of Open Access books Built by scientists, for scientists

4,800

Open access books available

122,000

International authors and editors

135M

Downloads

Our authors are among the

154

Countries delivered to

TOP 1%

most cited scientists

12.2%

Contributors from top 500 universities



WEB OF SCIENCE™

Selection of our books indexed in the Book Citation Index
in Web of Science™ Core Collection (BKCI)

Interested in publishing with us?
Contact book.department@intechopen.com

Numbers displayed above are based on latest data collected.

For more information visit www.intechopen.com



Climbing with Parallel Robots

R. Saltarén, R. Aracil, O. Reinoso¹ and E. Yime
 DISAM Universidad Politécnica de Madrid,

¹Departamento de Ingeniería de Sistemas Industriales, Universidad Miguel Hernández
 Spain

1. Introduction

Inherently, parallel robots present many advantages to climb in comparison with robots that use serial legs. The availability of a great number of redundant degrees of freedom on the climbing robots with legs does not necessarily increase the ability of those types of machine to progress in a complex workspace. The serial legs mechanisms have a sequential configuration that imposes high torques on the actuators placed on the base. Therefore, the architecture of serial legs of some climbing robots implies a limit on load capability. In contrast with the limitations of the climbing robots with legs, the use of a Gough–Stewart platform as a climbing robot (Stewart, 1965), solves many of these limitations and opens a new field of applications for this type of mechanism. In order to emphasize the great performance of the G–S parallel robot as a climbing robot, it is pertinent to remember that this type of parallel robot is based on a simple mechanical concept that consists of two rings (platforms) linked with six linear actuators joined through universal and spherical joints (this type of structure is also referenced as a 6-UPS parallel robot). These characteristics allow obtaining a mechanical structure of light weight and with high stiffness, which is able to reach high velocities and develop big forces with a very important advantage: the low cost of manufacturing (Lazard, 1992)). The forward kinematic of the G–S platform has been previously analyzed for many authors (Husty, 1994) (Dasgupta, 1994). This paper has been developed in based to references (Almonacid, 2003) (Aracil, 2003) (Aracil, 2006) and (Saltaren 2005) and reflects the state of the art of the researchers made by the authors during the last years.

The morphology proposed for the parallel G–S platform as climbing robot is shown in Fig. 1(a). The G–S platform is formed by two rings joined with 6 linear actuators as UPS kinematics chains (where the U degrees of freedom belong to a universal joint, P is a prismatic degree of freedom that belongs to the linear actuator and S is the spherical joint) (Saltaren, 2000). The robot assembly around the tubular structure is carried out through a system of hinges. The holding systems are based on a series of grip devices built in each ring. Those grip devices hold the reference ring firmly attached to the tubular structure while the free ring is displaced by the control system. In Fig. 1(b), we show the climbing robot to work on the outside wall of pipes. In this case the platform of Fig. 1(a) is modified by adding two legs on each one of the external rings of the robot. These legs allow fastening one ring to the pipe while the other ring moves along the structure. The external rings can rotate increasing the working space of the robot.

Source: Bioinspiration and Robotics: Walking and Climbing Robots, Book edited by: Maki K. Habib
 ISBN 978-3-902613-15-8, pp. 544, I-Tech, Vienna, Austria, EU, September 2007

To show the viability of the G-S platform as a climbing robot it is necessary to study the behaviour of this platform in some critical configurations of their movements along the inside and outside of tubular structures. In Fig. 2(a) we show a parallel robot climbing through a pipe rounding it with their rings and grasping with radial grip devices. This kind of robot is limited to tasks in which the tubular structure has low curvatures. In other case the linear actuators of the robot will collide with the tubular structure. Also we can evaluate some critical configurations when a parallel robot moves through the outside of tubular structures. In Fig. 2(d)–(f) we show a robot avoiding the obstacles of some tubular structures or pipes as corners, tees and valves. In each case, the robot must be able to climb with autonomy along a tubular structure and turn around, thanks to the implementation of a guidance system based in sensorial information. In some applications, the motion control system consists of a numerical path-planning algorithm which is based on the inverse and direct numerical kinematics (Aracil, 2000a) solution. In Fig. 2(b) and (c) we show a climbing parallel robot moving along the inside of tubular structures avoiding the collisions between the linear actuators and the surface of the structure. To achieve that this robot moves through the inside of the pipe, it is necessary to define an appropriate relation between the diameter of the rings of the robot, the maximum displacement between the rings and the diameter of the pipe.

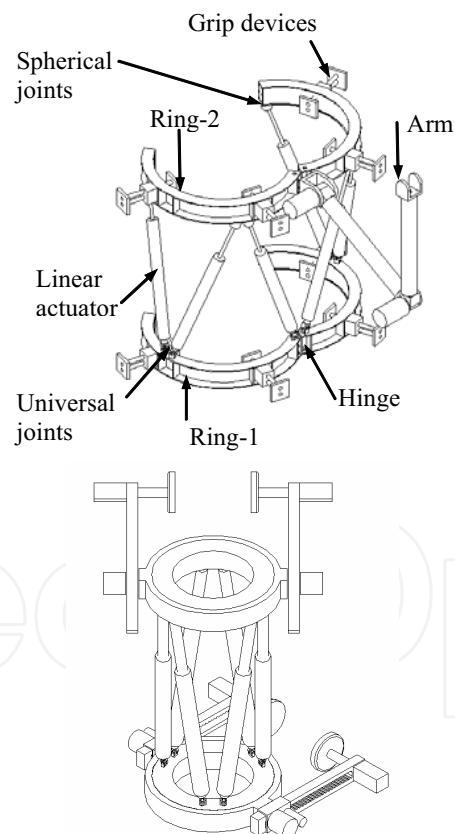


Figure 1. Functional concept: (a) mechanical design of the robot, (b) mechanical design of the robot with clamping legs to climb along the outside wall of pipes

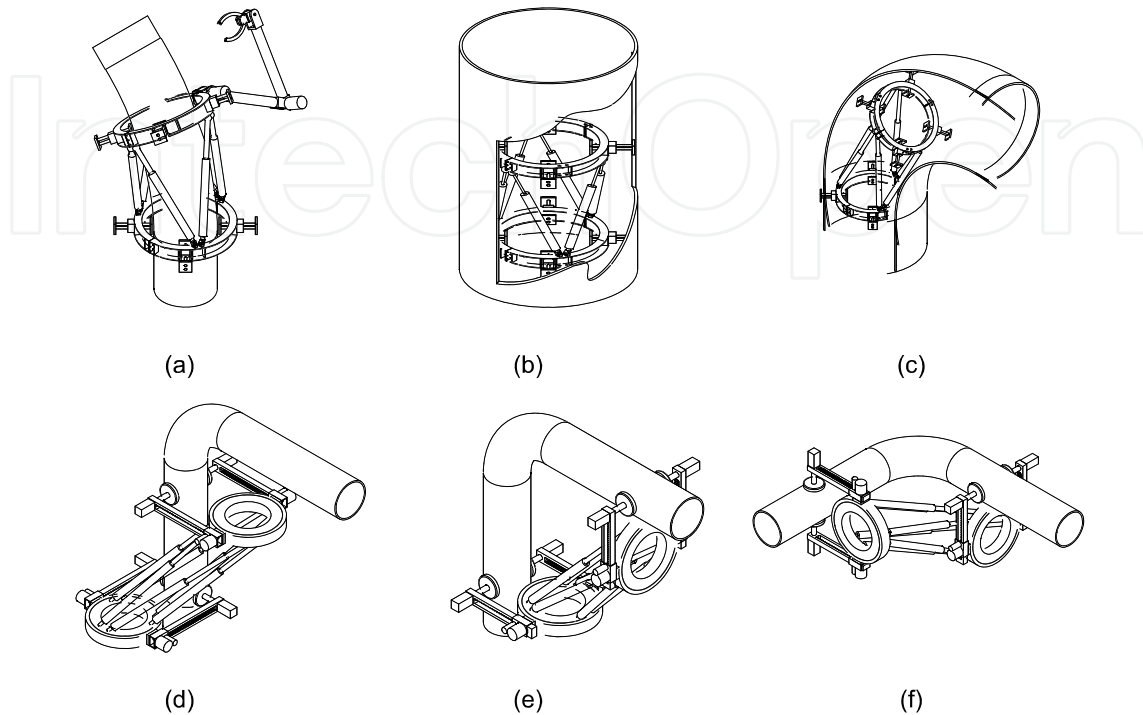


Figure 2. Parallel robots on pipes: (a) robot for working on cables and palm trees, (b), (c) robot for working on curves pipes and tubular structures, (d), (e), (f) some critical configurations of the robot

2. Design of Climbing Parallel Robot

S-G platforms can offer a solution of interest as mobile robots for the development of tasks on structural frames, such as those used in buildings. The use of S-G platforms as CPRs means a new approach that allows resolving some typical problems that can concern in the kinematic and dynamic behaviour of a robot climbing through complex structural frames. These questions are as follows.

1. A climbing robot must be capable of supporting its own weight and also the payload in its movements. Therefore, the robot should weigh as little as possible.
2. A climbing robot must adopt critical configurations to pass a structural node. These configurations depend on the way of the approximation to the structural node and on the direction that the robot must take, once the structural node has been overcome.
3. When a climbing robot works on structural frames, it must be capable of changing between working postures with a small number of movements.
4. Ideally, a climbing robot could use its power actuators in parallel to carry out the tasks and movements on structural frames. In this way, the power actuators can be of less power and, as a consequence, lighter.

3.1 Conceptual Design of the CPR

The morphology proposed for the CPR is based on a parallel platform of six degrees of freedom (DOFs). The main structure of the robot is similar to the classic structure of the parallel robot based on the S-G platform (Stewart, 1965) (Merlet, 1997). This platform consists of two parallel rings linked by six linear actuators as universal-prismatic-spherical (UPS) kinematic chains (where the U DOFs belong to an universal joint, P is a prismatic DOF that belongs to the linear actuator, and S is the spherical joint) (see Fig. 3). In the development of the CPR, it is necessary to carry out some modifications on this platform with the purpose of facilitating the movements of the robot on structural frames. The conceptual design of the robot used to climb along metallic structures is shown in Fig. 1. The robot is constituted by two cylindrical bases: a base or lower ring (Ring-1), and a base or upper ring (Ring-2). These two rings are linked by six linear actuators that allow the displacement between both bases. Over each one of the rings of the robot, an additional exterior rotating ring has been added, allowing turns off. In this way, the robot can orient its legs to facilitate the hold of the robot on the metallic structure. Previous prototypes of this robot have been developed to carry out tasks on pipes and tubular structures (Almonacid, 2003) (Aracil 2003). However, some changes have been added to previous platforms, due to the inherent features of the structural frames in which the robots must work. In contrast to the climbing robot presented in (Saltaren, 2000b) with an interior clamping device to hold and climb by palm trunks and pipes, the clamping devices of the robot to work on structural frames should fold and extend at least in two predetermined positions. The possibility of folding or extending the clamping legs allows reducing possible collisions between the movement ring and the environment. Moreover, in some sequences of displacement, it is necessary to orient the legs of each one of the rings of the robot to predetermined positions (-90° , 0° , $+90^\circ$), because the rotation of the exterior ring with its clamping device may reduce the rotation requirements of both rings around its axes. In this way, it is possible to avoid singular configurations of the parallel robot, reported by Fichter (Fichter, 2003). For the same reason, it is possible to avoid the collisions between the linear actuators originated when they cross themselves in the displacement of each one of the two rings of the robot.

3.2 Spherical and Universal Joints Adaptations

The robot needs to orient its rings at 90° to accomplish displacements through structural frames. So, with the purpose of allowing configurations of 90° between the rings that constitute the basis of the robot, the spherical and universal joints have been adapted with a new design (Fig. 4 (a), (b)). As we can observe in Fig. 4(b), the new suggestion of the universal joint consists of redesigning in cantilever the junction of the two parts of the classical universal joint.

The modified spherical joint is achieved, adding a rotation in the junction of the linear actuator with the universal joint. In Fig. 4(c), a detail of the new modified joints added to the robot is illustrated. With these new joints, the robot can achieve all the necessary postures to carry out the required displacements detailed in the following section. The image shows that the robot can reach configurations of 90° between its rings with the new modified joints.

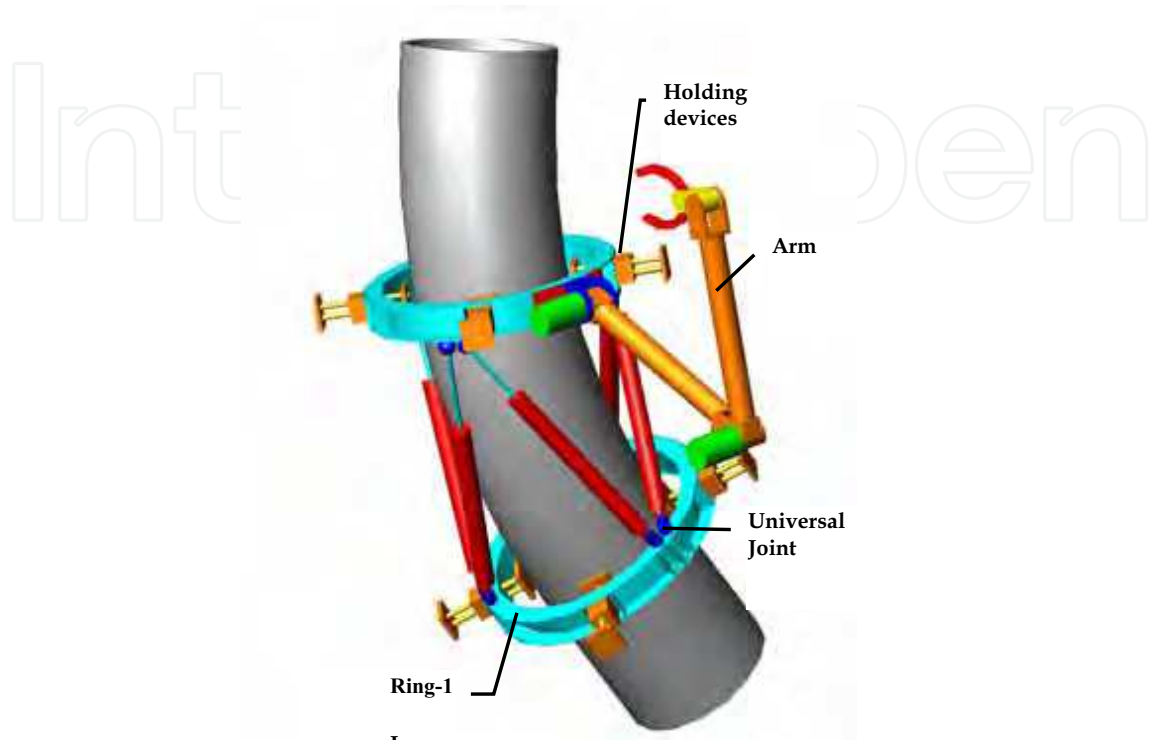


Figure 3. Climbing Parallel Robot

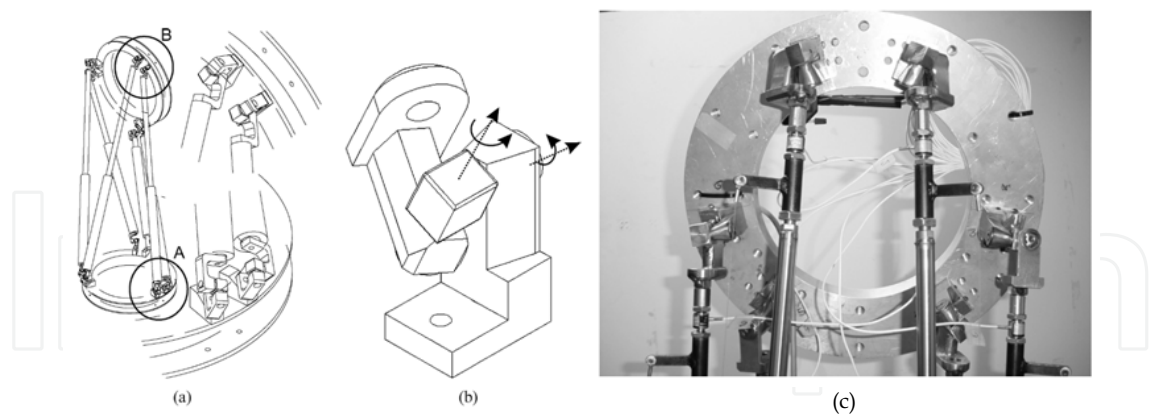


Figure 4. To accomplish postures of 90° between both rings of the robot, it is necessary to modify the spherical and universal joints. (a) Details A and B indicate the necessity of open spherical and universal joints to achieve the orientations between the rings. (b) Modified joints are shown. (c) Upper ring is at 90° with respect to the lower ring, using the modified universal joints

3. Modeling and Analysis of the Jacobian of the CPR

The singularities of a parallel robot come determined by the determinant of the Jacobian, thus the first step to analyze such singularities consists of calculating the Jacobian that represents the kinematic behaviour of the CPR in the different postures. The Jacobian of the Stewart platform is specified using the reciprocal screws theory and employing the nomenclature of Fig. 5. This Jacobian is based in a reference system localized in the upper ring. For the CPR proposed in the previous section, we propose the use of a variation of this model. In our case, we use the lower platform as the basis for the formulation. Taking into account Fig. 5, a CPR is constituted by six kinematic UPS chains. Each one of these kinematic chains is made up by a linear actuator and their mechanical connections to the upper and lower ring through U, P (actuator), and S joints.

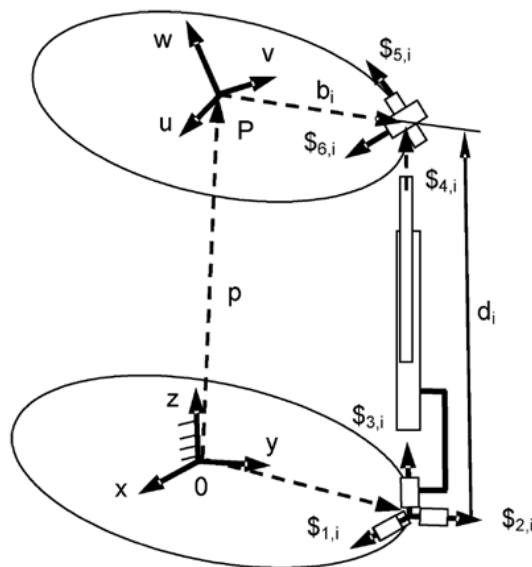


Figure 5. Nomenclature of the CPR to calculate the Jacobian

From Fig. 5, we have the following.

- a_i Array from the middle of the lower ring to the middle of each U joint.
- b_i Array from the middle of the upper ring to the middle of each S joint.
- p Array from the middle of the lower ring to the middle of the upper ring.
- d_i Array from the middle of the U joint to the middle of the S joint in each actuator.
- $\$_{n,i}$ Unit screws through each link.

If all the screws take as reference the middle of the lower ring, the following unitary screws can be derived for each link:

$$\begin{aligned}
\hat{\$}_{1i} &= [u_{1,i}^T - u_{1,i}^T \tilde{a}]^T \\
\hat{\$}_{2i} &= [u_{2,i}^T - u_{2,i}^T \tilde{a}]^T \\
\hat{\$}_{3i} &= [0_{1 \times 3} u_{3,i}^T]^T \\
\hat{\$}_{4i} &= [u_{4,i}^T - u_{4,i}^T (\tilde{a} + \tilde{d})]^T \\
\hat{\$}_{5i} &= [u_{5,i}^T - u_{5,i}^T (\tilde{a} + \tilde{d})]^T \\
\hat{\$}_{6i} &= [u_{6,i}^T - u_{6,i}^T (\tilde{a} + \tilde{d})]^T
\end{aligned} \tag{1}$$

where $u_{n,i}$ is the unitary array of the kinematic chain for the unitary screw of the link . So, the resultant screw for each kinematic chain (linear actuator) is:

$$\begin{aligned}
T(p)\$_{ef} &= \omega_{1,i} \hat{\$}_{1,i} + \omega_{2,i} \hat{\$}_{2,i} + \omega_{3,i} \hat{\$}_{3,i} \\
&\quad + \omega_{4,i} \hat{\$}_{4,i} + \omega_{5,i} \hat{\$}_{5,i} + \omega_{6,i} \hat{\$}_{6,i}
\end{aligned} \tag{2}$$

where $T(p)$ is the transformation matrix between points, and $\omega_{j,i}$ is the angular velocity array for the screw. On the other hand, the reciprocal screw to the screws $\$_{1,i}, \$_{2,i}, \$_{3,i}, \$_{4,i}, \$_{5,i}$ and $\$_{6,i}$ is

$$\hat{\$}_{rec,i} = [u_{3,i}^T - u_{3,i}^T \tilde{a}]. \tag{3}$$

Using the Klein product between the reciprocal screw (3) and the screw for the end-effector (2), we can derive six equations that formulate the relation between the velocity of the end-effector and the velocity of the actuators

$$\begin{bmatrix} v_1 \\ v_2 \\ v_3 \\ v_4 \\ v_5 \\ v_6 \end{bmatrix} = \begin{bmatrix} -(\tilde{u}_{3,1}(\mathbf{a}_1 - \mathbf{p}))^T & \mathbf{u}_{3,1}^T \\ -(\tilde{u}_{3,2}(\mathbf{a}_2 - \mathbf{p}))^T & \mathbf{u}_{3,2}^T \\ -(\tilde{u}_{3,3}(\mathbf{a}_3 - \mathbf{p}))^T & \mathbf{u}_{3,3}^T \\ -(\tilde{u}_{3,4}(\mathbf{a}_4 - \mathbf{p}))^T & \mathbf{u}_{3,4}^T \\ -(\tilde{u}_{3,5}(\mathbf{a}_5 - \mathbf{p}))^T & \mathbf{u}_{3,5}^T \\ -(\tilde{u}_{3,6}(\mathbf{a}_6 - \mathbf{p}))^T & \mathbf{u}_{3,6}^T \end{bmatrix} \begin{bmatrix} w_x \\ w_y \\ w_z \\ v_x \\ v_y \\ v_z \end{bmatrix} \tag{4}$$

or, in matrix notation

$$\mathbf{v} = J\$_{ef}. \tag{5}$$

This equation can be rewritten as

$$v = J_{rec} T(p) \$_{ef} \tag{6}$$

where J_{rec} is the Jacobian made up for the reciprocal screws to each kinematic chain that are represented by the system referred to the middle of the lower ring

$$J_{rec} = \begin{bmatrix} (\Delta_{rec,1})^T \\ \vdots \\ (\Delta_{rec,6})^T \end{bmatrix}. \quad (7)$$

4. Parallel Robots for Climbing Tubular Structures

The use of Stewart-Gough (S-G) platform as climbing robots (CPR) to perform tasks in tubular structures such as oil pipes, bridge steel cables, towers and trunks of palm trees is very promising (Aracil, 2003).

Mechanical adaptation is the first aspect to be solved in developing a CPR. As shown in figure 3, it is necessary to divide the two rings into two parts that are connected by a hinge and a lock with a clamping device so that the S-G platform can adapt to climb outside the tube. By such manner, it allows the CPR to be assembled on the tubes as shown in figure 6. It also allows the gripping system to be attached in every ring so as to hold out upon displacement inside the tube (Aracil, 2000). The gripping system for holding out is radial to the rings as observed in figure 6, cases (a) and (c). Undoubtedly, the most important adaptation is redesigning of the robot universal joints. It is necessary to design a special universal joint that is capable to have big rotations as observed in figure 6 (b). These joints should be more mechanically robust in contrast to the standard universal joints.



Figure 6. Mechanical adaptation of an S-G platform

4.1 Morphology of robots for climbing Tubes

CPRs can climb along exterior and interior of tubes. These two possibilities in its displacement are as follows:

1. Such displacement has already been fore mentioned in figure 3. It consists of holding around the tube and moving up by using grips attached to the rings. It displaces along the tube as one ring holds up and the other free ring moves on. In similar manner, CPRs can be used to climb inside tubular structures as shown in figure 2 (c). This mentioned robot can move its rings along the curve of a tube through a system that controls the centering of the rings.

2. The other manner of climbing is shown in figure 7. Two arms that can extend and retract are connected to each ring and serve as holding device. This kind of robot works when climbing outside tubular structures with obstacles due to its structural design.

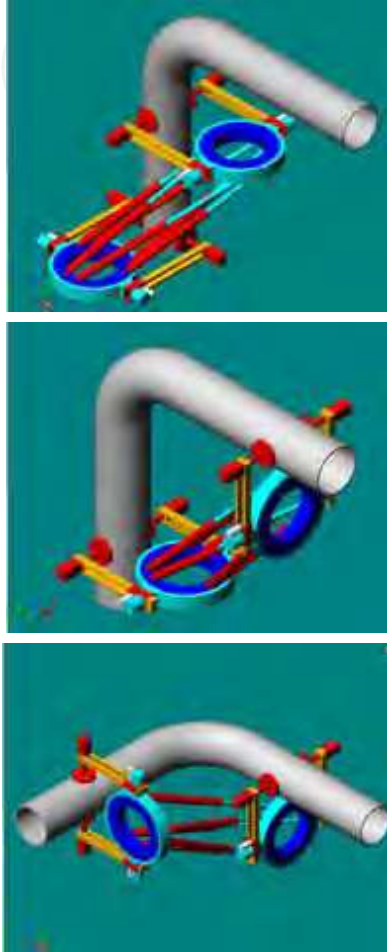


Figure 7. CPR robot climbing outside tubular structures

4.2 Applied case: Robot to climb along palms trees

To show the climb with parallel robots, a CPR prototype called TREPA has been developed to climb along trunks of palm trees with the objective of trimming branches and fumigation (Aracil, 2006), (Saltaren 2005). Palm trees are very common in the Mediterranean coast and grow as high as 18 to 22 meters. Currently, most palm trees on the Spanish Mediterranean coastlines are affected by disease. The problem is difficult to control as there is a lack of expert operators that can climb the palm trees to trim up the branches and spray out insecticide. The automation of such type of task is an excellent alternative due to the danger and risk of falling from such height and getting contaminated from the insecticide.

4.3 Algorithms for CPR in tubular structures

The automatic control of a robot that climbs along tubular structures should take into account geometrical changes in the path of the tubes. As a consequence, three 120° ultrasonic sensors have been installed in every ring of the TREPA robot. The three sensors allow calculating the difference between the center of the ring and the tube (Aracil, 2003).

Based on this estimate, an algorithm to control the displacement of the moving ring can be done by maintaining it centered and following the curve of the tube automatically (Almonacid, 2003). In this context, the inverse and direct kinematics problems need to be solved as well, so as to control the automatic climbing of a CPR along a pipe. A brief description about a climbing cycle that explains the compromise between two solutions of kinematics is shown as follows.

1. At the beginning of a climbing process, for example, the lower ring is held onto the tube by its clamping system as shown on the sequence explained in figure 4.
2. The actual configuration of the robot with respect to the reference system of the lower ring can be determined by means of the trajectory control algorithm as shown in figure 9 using the direct kinematics solution.
3. According to the actual configurations of the robot (with the system of reference in the lower ring), the total path of the center of the ring (upper ring) is calculated through pipe line and this path is divided in steps. Based on inverse kinematics solution, displacement of each linear actuators is calculated; $C_i = (C_1, C_2, C_3, C_4, C_5, C_6)$. From the beginning of the cycle and every time the upper ring passes through a step of the path, the centering of the ring is automatically corrected based on the measurements of the ultrasonic sensors. This action is done by the path control algorithm. Besides this correction, adjustment on the orientation of the ring is done by the algorithm.
4. While the upper ring is displaced and before the ring moves forward to the next step, the validity of displacement is verified by an analysis of singularity through robot Jacobian. In case of a singularity, the next movement is cancelled. The mobile ring clamps up and the new configuration is calculated through direct kinematics. While doing so, both rings are holding up.
5. Based on the calculated configuration of the robot as previously mentioned, the reference frames of the rings are interchanged. It takes the upper ring as new system of reference and goes back to step 1 to pull the lower ring.

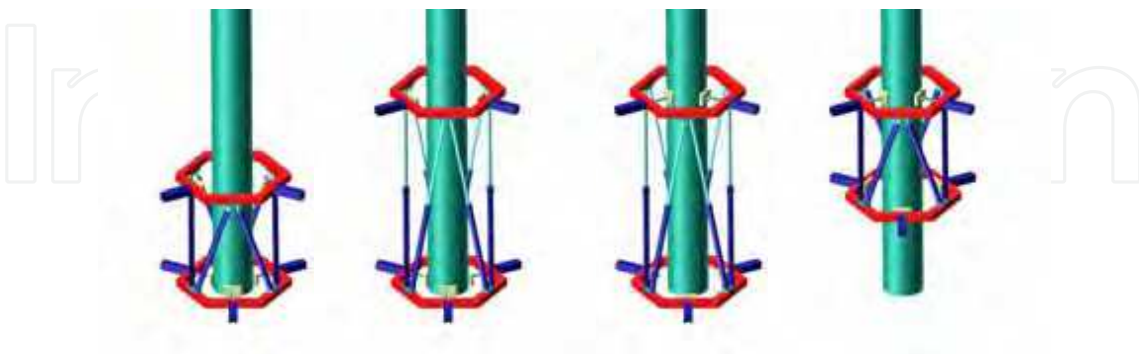


Figure 8. Steps that define the climbing process of a CPR

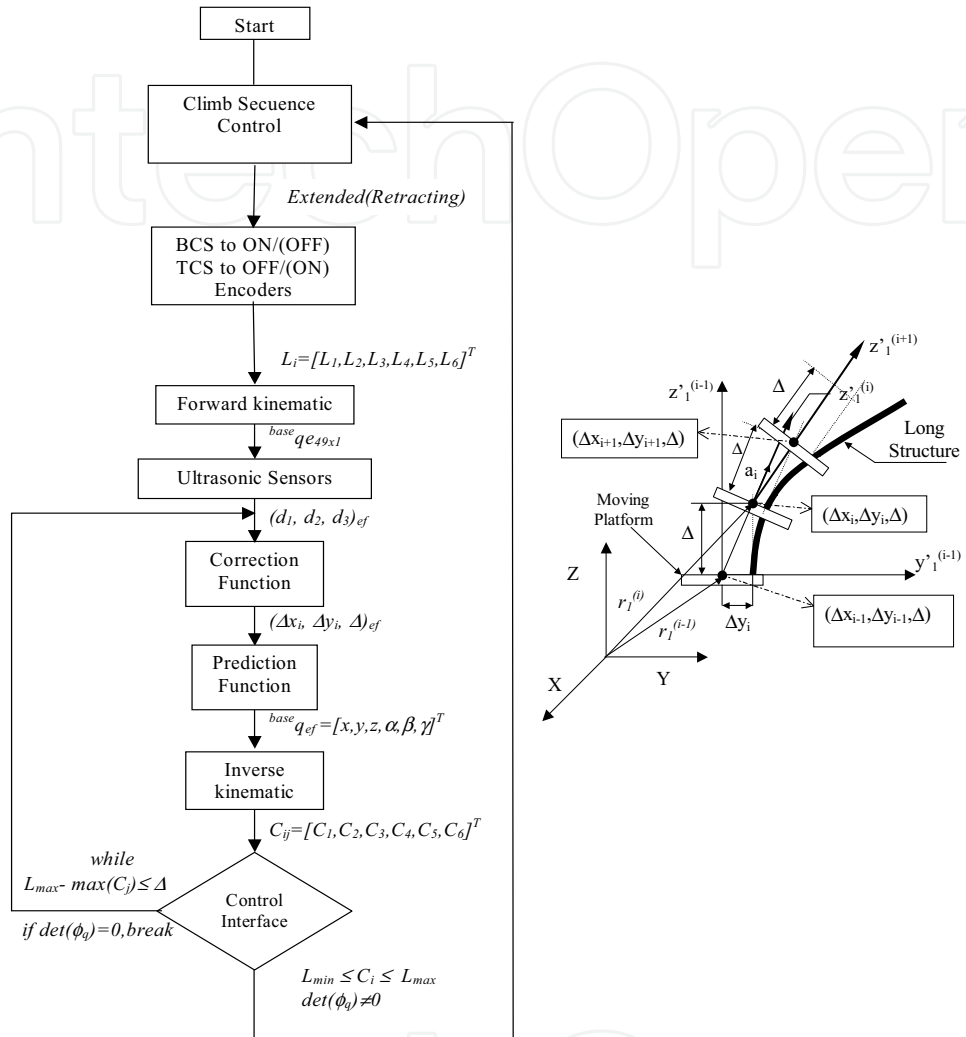


Figure 9. Algorithm to climb up



Figure 10. Climbing sequence experimental results

Figure 10 shows a sequence of images of the prototype for the TREPA robot. It has 6 pneumatic cylinders. Every cylinder is controlled through a proportional valve FESTO MPYE-5. A linear encoder measures its displacement. The gripping system, which is activated pneumatically, can be seen in every ring. A multi-axis Delta Tau PMC-VME card has been used for the control structure of the robot. In figure 10 some images of the parallel robot climbing on a palm trunk are shown. The images show the robot in different positions of the palm trunk. The first version of the prototype designed to climb this kind of structures moves to a velocity of 0.4 m/s.

5. Parallel Robots to Climb Along Structural Frames

To climb along metallic structures, one of the two rings of the CPR robot must be considered as final effector, depending on the direction of displacement. The solution can be obtained from the vectorial description on generalized coordinates, and it is extensively reported in (Almonacid, 2003). Taking into account the inverse kinematic solution, a path planning for the dynamic analysis of the sequence of the robot displacement has been carried out. As Fig. 11 shows, the robot can accomplish the movement through the displacement of ring 2 with regard to ring 1, together with adequate movements in the clamping system. This displacement is composed of four steps.

1. The CPR grasps the beam with both ring legs.
2. The robot is held by ring 1 legs. Ring 2 legs are released and folded. Linear actuators are commanded, allowing ring 2 to acquire the required position.
3. The ring that has been displaced (ring 2) is held through its clamping devices.
4. With ring 2 grasping the beam, ring 1 is released. Ring 1 acquires the new position.

Once ring 1 has achieved the position, the robot is ready for a new cycle.

As Fig. 11 shows, to generate movements through the right path, the postures that the robot must achieve are simple and easily reachable. However, when it is necessary to generate movements that allow the robot to climb through a metallic structure and to pass its structural nodes, different postures can be demanded. Furthermore, such postures need to be analyzed. We denote as structural node three beams making a corner. In such structural nodes, the robot can change the direction of its movement, or can keep the same direction when passing them.

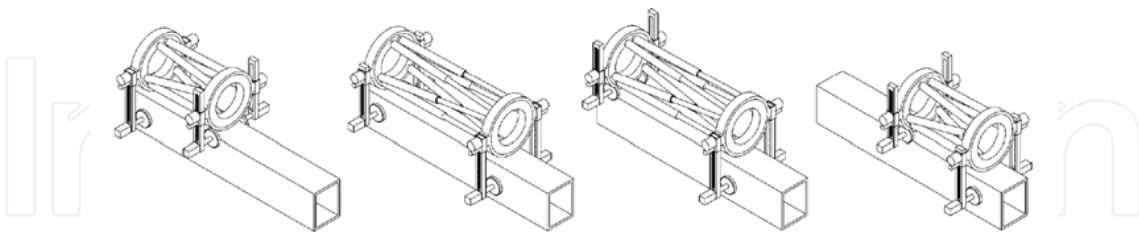


Figure 11. Sequence of the displacements of the robot along a straight trajectory

5.1 Sequence to Evade a Structural Node

The postures that a CPR can achieve to pass a structural node are presented in Fig. 12. The achievement of one posture among them depends on the direction that the robot must take

to follow the path once the structural node has been passed. In Fig. 13, an example of a sequence of postures is shown. This sequence shows that a CPR requires a minimum number of postures to pass a structural node.

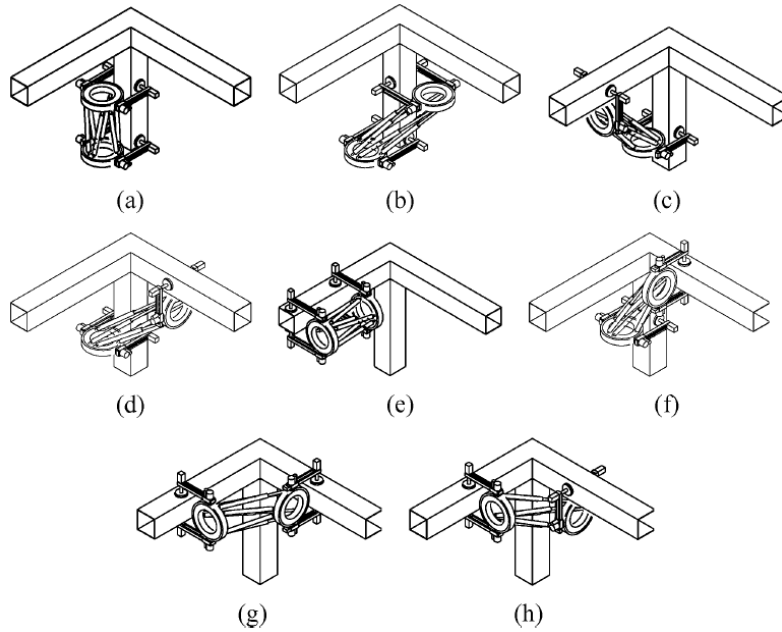


Figure 12. Analysis of the climbing sequences used in order to evade a structural node. (a) Initial posture Pos-1. (b) Final posture Pos-1a. (c) Final posture Pos-1b. (d) Final posture Pos-1c. (e) Final posture Pos-1d. (f) Initial posture Pos-2. (g) Final posture Pos-2a. (h) Final posture Pos-2b

In the following section, a simulated dynamic analysis, considering several configurations that the robot can achieve to pass the structural node, is discussed. In this analysis, we have considered different displacements of the robot, and also several sizes of the robot, with the purpose of obtaining valid conclusions about the features and dimensions more adequate for a CPR working on structural frames. Previous to making the dynamic analysis of the CPR robot, it is necessary to study possible configurations that the robot can achieve to evade a structural node. Some of these configurations are close to singular configurations. For this reason, the Jacobian in the orientation workspace needs to be evaluated.

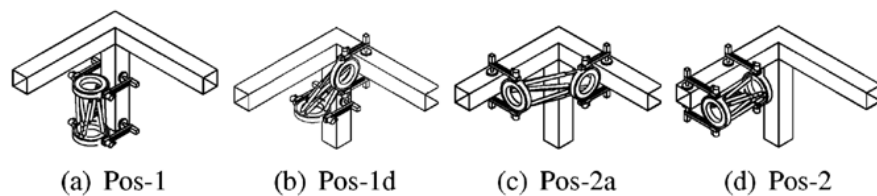


Figure 13. Sequence of postures evading a structural node

6. Dynamic Simulation and Analysis of Three Types of CPR

The dynamic analysis of some postures of the CPR is developed in this section. This analysis is essential to show that the CPR robot is feasible from the mechanical point of view. The mechanical feasibility of the CPR can be considered if the forces on the linear actuators are reasonable. The forces that affect a CPR near of the end of each posture may be very elevated, because the upper ring is moving near singular configurations. We study this aspect in two steps. First, we develop a computational analysis about the dynamics performance of three types of CPR. This analysis is required for the study of the tendency in the forces that affect each posture, and its relation to the size, payload, and the velocity of the robot. In a second step, we develop a robot testbed with the purpose of acquiring experimental data that allows us to contrast the computational results with the experimental results. The experimental studies have been made for four postures and for seven intermediate configurations, with the upper ring oriented to 90° with respect to its base. The experimental studies will be developed in the next section. So, three CPRs with different geometrical features have been considered in the dynamic simulations. The geometrical features of the CPRs are detailed in Table 1. The purpose of the simulations is analyzing the dynamic effects present in a CPR when the robot achieves some postures, taking into account its dimensions and velocity of displacement. Particularly, three kind of robots have been considered, and denoted as D150, D250 and D350, with a total weight of 20.5, 25.5, and 31.0 kg, respectively. The total weight of each robot corresponds to the weight of each one of the rings plus the weight of the six linear actuators plus the weight of the clamping devices.

Robot	Part	Unitary Weight (Kg)	Dim (mm)
D150	Ring-1 and Ext. Ring	2.75	ϕ :150
	Ring-2 and Ext. Ring	2.75	ϕ :150
	Linear actuators	6*1.50	ϕ :30, L:400
	Clamping Devices	4*1.50	L:250
	Total weight D150: 20.50 Kg		
D250	Ring-1 and Ext. Ring	3.50	ϕ :250
	Ring-2 and Ext. Ring	3.50	ϕ :250
	Linear actuators	6*1.75	ϕ :30, L:450
	Clamping Devices	4*200	L:300
	Total weight D250: 25.50 Kg		
D350	Ring-1 and Ext. Ring	4.50	ϕ :350
	Ring-2 and Ext. Ring	4.50	ϕ :350
	Linear actuators	6*2.00	ϕ :30, L:550
	Clamping Devices	4*2.50	L:350
	Total weight D350: 31.00 Kg		

Table 1. Physical parameters of the simulated robots

A set of dynamic simulations for previous robots D150, D250, and D350 (whose features are illustrated in Table I) have been carried out. The diameter of the rings of the robots is 150,

200, and 350 mm, respectively. Dynamic simulations have been carried out taking into account three different velocities, with the purpose of analyzing the forces required in the actuators to achieve the predefined posture. The velocities considered are 0.4, 0.6, and 1.0 m/s. Also, we have considered different payloads (50, 100, 150, and 200 N). The parameters used in the simulations for the path-planning sequences are shown in Table 2.

Seq.	Robot type		
	D150[mm, °]	D150[mm, °]	D150[mm, °]
Pos-1a	[-230,230,450,0,0,0]	[-270,270,500,0,0,0]	[-300,300,600,0,0,0]
Pos-1b	[450,0,450,90,-90,-90]	[500,0,500,90,-90,-90]	[600,0,600,90,-90,-90]
Pos-1c	[0,450,450,0,-90,0]	[0,500,500,0,-90,0]	[0,600,600,0,-90,0]
Pos-1d	[-230,450,450,0,-90,0]	[-270,500,500,0,-90,0]	[-200,600,600,0,-90,0]

Table 2. Parameters of displacements and 3-1-3 Euler angles

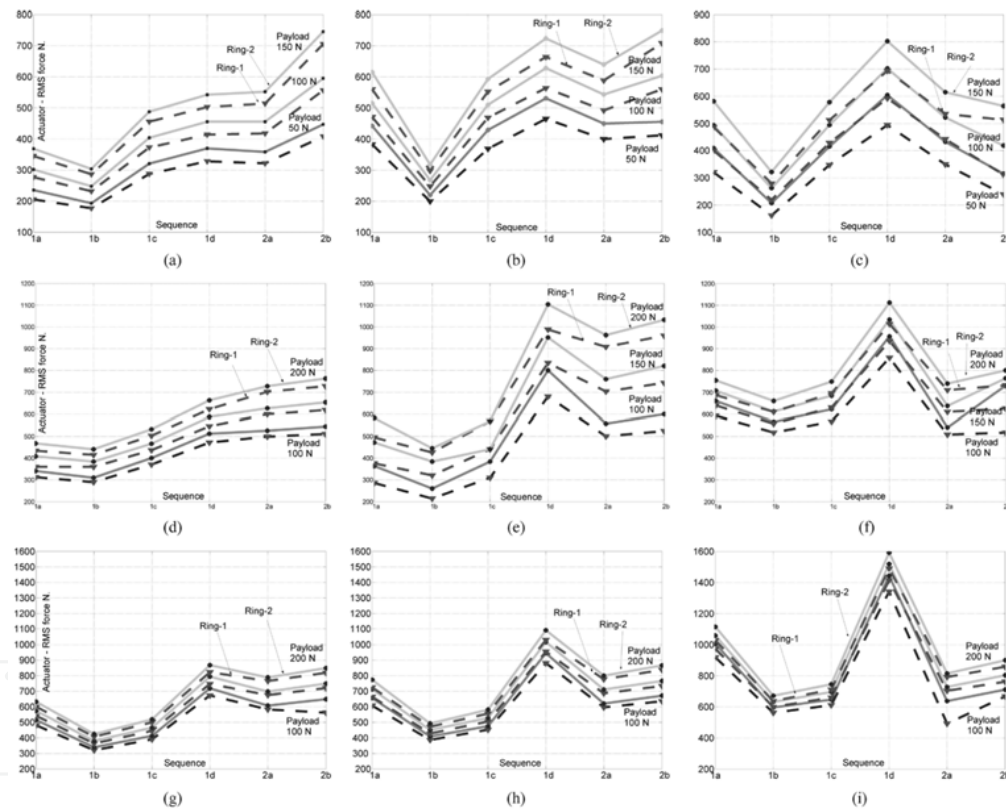


Figure 14. Results of the dynamic simulations for the calculation of the maximum RMS force (N) of the linear actuator under the largest burden. Each figure has three curves for the simulated velocities of 0.4, 0.6, and 1.0 m/s. Each one of the curves reflects the forces for the six different postures of the robot, as shown in Fig. 5. (a) D150 Vel: 0.4 m/s. (b) D150 Vel: 0.6 m/s. (c) D150 Vel: 1.0 m/s. (d) D250 Vel: 0.4 m/s. (e) D250 Vel: 0.6 m/s. (f) D250 Vel: 1.0 m/s. (g) D350 Vel: 0.4 m/s. (h) D350 Vel: 0.6 m/s. (i) D350 Vel: 1.0 m/s

Results of the simulations are shown in Fig. 14. Each one of the graphics in this figure can be explained as follows.

1. The horizontal axis on each graphic corresponds to the postures Pos-1a, Pos-1b, Pos-1c, Pos-1d, Pos-2a, and Pos-2b. The vertical axis corresponds to the force required in the actuator (in Newtons).
2. Each graphic has three pairs of curves that correspond to the payloads of the robot. Each payload comprises
3. two curves: one for the displacement of the upper ring, and the other one for the displacement of the lower ring. The weight of the rings is not the same, because we have considered the weight of the servos of the linear actuators that are assembled at the end of the linear actuator.
4. The curves have been created evaluating for each posture the maximum root mean square (RMS) force of the more requested linear actuator. For example, for the case of the D150 robot and for a velocity of 0.4 m/s and a payload of 150 N, the maximum RMS force is requested in posture Pos-1d (500 N), considering ring 1 fixed and displacing ring 2.

6.1 Discussion of the simulation results

In this section, the results of simulations made to study the dynamic behavior of the robot in its displacement from an initial position to reach each posture in Fig. 12 are presented. These simulations have been carried out with ADAMS (Adams). Numerous simulations have been carried out with the aim of studying the dynamic performance of the CPR. From Fig. 14, we can observe that for a 0.6 m/s velocity (b,e,h), and for a 1.0 m/s velocity (c,f,i), the displacement of sequence 1d in Fig. 12 requires larger forces in linear actuators. Using the results from Fig. 13, it can be observed that the dynamic results that give rise to the most uniform forces among the six different postures evaluated correspond to the velocity of 0.4 m/s. It is clear that the dynamic performance of the CPR is affected by the magnitude of its displacement sequence and payload, but more strongly by the velocity.

Posture	D150	D250	D350	Velocity (m/sec)
Pos-2b	740	800	860	0.4
Pos-1d	750	1100	1100	0.6
Pos-1d	800	1120	1600	1.0

Table 3. Example of maximum forces (in Newton) required by the most requested actuator

From Fig. 12, it can be deduced that for D250 and D350 robots and for 0.6 and 1.0 m/s velocities, sequence 1d is the one that originates higher forces on the linear actuators. Some results of the RMS power, calculated following the data obtained for the higher RMS forces on each one of the cases in Fig. 14, are presented in Table 3. For example, taking into account the values of such graphics, we can deduce the posture Pos-1d as most critical, from a dynamic point of view, when the payload is 200 N. It would be approximately necessary to have a maximum force of 1120N by actuator. Other values of maximum forces required to reach the analyzed postures can be deduced from data presented in Fig. 14, taking into account the payload and the velocity of the robot. However, it can be concluded that posture Pos-1d requires maximum forces in the actuators.

7. Conclusion

The S-G platform with proper mechanical adaptation could be used for a CPR robot. A CPR has great advantages compared to a serial robot with legs. Advantages, such as high weight payload capacity, are obtainable since the final effectors of the robot are directly connected in parallel to the base through the linear actuators. Consequently, a heavy weight load capacity is essential for a climbing robot, as it must consider carrying its deadweight as well. Weight restriction slows down advancement in the development of climbing robots. The results obtained are quite promising in many ways.

1. First, a parallel robot mechanism is simple and robust. Its deadweight is less than that of a serial robot designed to perform similar tasks.
2. The simplicity of the parallel robot's mechanical design is excellent; as it has two rings connected by six linear actuators through universal and spherical joints.

The CPR has overcome two main difficulties. The first is related to the task of climbing along tubes or trees. The development of the experimental prototype and the results show that the parallel robot is able to climb along tubes and stems. This capability is highly regarded when the parallel robot is able to adapt to the structural changes and get around performing its task. The second difficulty is related to climbing structures. The design of climbing robots for structures has 6 DOF; it allows one of the two rings to orient and displace conveniently and hold onto the rails of the metallic structure. To overcome the structural node, the robot must complete some postures that are relatively simple compared to other types of climbing devices. Some problems of singularity in certain orientations inside the working space of the robot can arise. But, on the whole, the climbing sequences and four postures previously mentioned are attainable. In conclusion, CPRs have great advantages that make them more promising than other climbing robots. Some research work in the teleoperation for these devices is being done, along with development of algorithms that will operate the robots semiautomatically in their trajectory when they displace along the tubular or metallic structure.

8. References

- ADAMS-10.0. Software simulation a reality, MDI
- Almonacid, M. ; Saltaren, R. ; Aracil, R. & Reinoso, O. (2003). *Motion planning of a climbing parallel robot*, IEEE Transactions on Robotics and Autonomous Systems, Vol. 19, No. 3, pp. 485-489
- Aracil, R. ; Saltaren R. ; Almonacid, M. ; Sabater, J.M. & Azorin, J.M. (2000). *Kinematic control for navigation of mobile parallel robots applied to large structures*, International Symposium on Automation and Robotics in Construction
- Aracil, R. ; Saltaren, R. & Reinoso O. (2003). *Parallel robots for autonomous climbing along tubular structures*, Robotics and Autonomous Systems, Vol. 42, No. 2, pp. 125-134
- Aracil, R. ; Saltaren, R. & Reinoso, O. (2006). *A Climbing Parallel Robot: A robot to climb along tubular and metallic structures*, IEEE Robotics & Automation Magazine, Vol. 13, No. 1, pp. 16-22
- Dasgupta, B. ; Mruthyunjaya, T.S. (1994). *A canonical formulation of the direct position kinematics for a general 6-6 Stewart platform*, Mechanism and Machine Theory, Vol. 29, No. 6, pp. 819-827

- Fichter, E.F. (2003). *A Stewart platform-based manipulator: General theory and practical consideration*, The International Journal of Robotics Research, Vol. 5, No. 2, pp. 125-134
- Husty, M. L., (1994). An algorithm for solving the direct kinematic of Gough-Stewart type platforms, *Rapport de Recherche TR-CIM-94-7*, Univ. McGill, Montreal
- Merlet, J. (1997). *Les robots paralleles*, Ed. Hermes
- Lazard, D. (1992). *Stewart Platform and Grobner basis*, In ARK Ferrae, pp. 136-142
- Saltaren, R. ; Aracil, R. ; Reinoso, O. ; Sabater, J.M. & Almonacid M. (2000a). *Parallel climbing robot for construction, inspection and maintenance*, International Symposium on Automation and Robotics in Construction, Madrid, pp. 359-364
- Saltaren, R. ; Sabater, J.M. ; Azorin, J.M. ; Reinoso, O. & Aracil, R. (2000b). *Research and development of a pneumatic control for a parallel climbing robot*, CLAWAR'2000 Climbing and Walking Robots, Madrid, Spain, pp. 461-475
- Saltaren, R. ; Aracil, R. ; Reinoso, O. & Scarano, M.A. (2005). *Parallel Robot: A computational and experimental study of its performance around structural nodes*, IEEE Transactions on Robotics, Vol. 21, No. 6, pp. 1056-1066
- Stewart, D. (1965). *A platform with six degrees of freedom*, Proc. Instn Mech. Engrs (Part I), pp. 371-38



Bioinspiration and Robotics Walking and Climbing Robots

Edited by Maki K. Habib

ISBN 978-3-902613-15-8

Hard cover, 544 pages

Publisher I-Tech Education and Publishing

Published online 01, September, 2007

Published in print edition September, 2007

Nature has always been a source of inspiration and ideas for the robotics community. New solutions and technologies are required and hence this book is coming out to address and deal with the main challenges facing walking and climbing robots, and contributes with innovative solutions, designs, technologies and techniques. This book reports on the state of the art research and development findings and results. The content of the book has been structured into 5 technical research sections with total of 30 chapters written by well recognized researchers worldwide.

How to reference

In order to correctly reference this scholarly work, feel free to copy and paste the following:

R. Saltaren, R. Aracil, O. Reinoso and E. Yime (2007). Climbing with Parallel Robots, Bioinspiration and Robotics Walking and Climbing Robots, Maki K. Habib (Ed.), ISBN: 978-3-902613-15-8, InTech, Available from:

http://www.intechopen.com/books/bioinspiration_and_robotics_walking_and_climbing_robots/climbing_with_parallel_robots

INTECH
open science | open minds

InTech Europe

University Campus STeP Ri
Slavka Krautzeka 83/A
51000 Rijeka, Croatia
Phone: +385 (51) 770 447
Fax: +385 (51) 686 166
www.intechopen.com

InTech China

Unit 405, Office Block, Hotel Equatorial Shanghai
No.65, Yan An Road (West), Shanghai, 200040, China
中国上海市延安西路65号上海国际贵都大饭店办公楼405单元
Phone: +86-21-62489820
Fax: +86-21-62489821

© 2007 The Author(s). Licensee IntechOpen. This chapter is distributed under the terms of the [Creative Commons Attribution-NonCommercial-ShareAlike-3.0 License](https://creativecommons.org/licenses/by-nc-sa/3.0/), which permits use, distribution and reproduction for non-commercial purposes, provided the original is properly cited and derivative works building on this content are distributed under the same license.

IntechOpen

IntechOpen